

Article

Manipulation of Unknown Objects to Improve the Grasp Quality Using Tactile Information

Andrés Montaña  and Raúl Suárez * 

Institute of Industrial and Control Engineering (IOC), Universitat Politècnica de Catalunya (UPC), 08028 Barcelona, Spain; andres.felipe.montano@upc.edu

* Correspondence: raul.suarez@upc.edu; Tel.: +34-93-401-6548

Received: 20 March 2018; Accepted: 18 April 2018; Published: 3 May 2018



Abstract: This work presents a novel and simple approach in the area of manipulation of unknown objects considering both geometric and mechanical constraints of the robotic hand. Starting with an initial blind grasp, our method improves the grasp quality through manipulation considering the three common goals of the manipulation process: improving the hand configuration, the grasp quality and the object positioning, and, at the same time, prevents the object from falling. Tactile feedback is used to obtain local information of the contacts between the fingertips and the object, and no additional exteroceptive feedback sources are considered in the approach. The main novelty of this work lies in the fact that the grasp optimization is performed on-line as a reactive procedure using the tactile and kinematic information obtained during the manipulation. Experimental results are shown to illustrate the efficiency of the approach.

Keywords: robotic manipulation; grasping; grasp quality; tactile sensors; tactile manipulation

1. Introduction

Object manipulation is a common task in service and industrial robotics. The development of complex robotics hands has impeded the search of manipulation strategies to take advantage of this hardware resource [1]. One of the common features of the new robotic hands is the inclusion of tactile sensors that allow to get information about the contacts with the manipulated object, increasing the robot capabilities. Usually, in a realistic scenario, the geometric model of the manipulated object is only partially known or even unknown. Tactile sensors help to recognize the manipulated object or to reduce the uncertainty in their geometric model.

The object manipulation process usually pursues three goals [2], either independently or in a combined way:

- From the hand point of view, the optimization of the hand configuration, i.e., searching for a particular hand configuration satisfying some specific constraints that can be arbitrarily defined.
- From the grasp point of view (relation hand-object), the optimization of the grasp quality, i.e., searching for a grasp that can resist external force perturbations on the object.
- From the object point of view, the optimization of the object configuration, i.e., searching for an appropriate object position and orientation that satisfy the requirements of a given task.

In order to manipulate an object, the first step is grasping it. Different grasp synthesis approaches have been proposed for known and unknown objects [3], but, in general, most of the grasp planners require an exact model of the object. Some approaches generate a set of feasible grasps and then choose the one that maximizes a quality metric [4–6], and others use a kinematic formulation of the grasp synthesis problem considering simultaneously the grasping constraints [7]. Other works look

for the grasping points on the object surface without considering the hand constraints, for instance, using geometric reasoning to find an optimal [8] or at least a valid grasps [9], or using an initial random grasp (that could not satisfy any quality criterion) to start a search of a valid or an optimal one either for single bodies [10] or for articulated objects [11]; these approaches require the evaluation of the grasp reachability for the used hand. Using tactile and visual feedback the planner can compute the grasp and adapt it to address problems such as slippage, the effect of external disturbances and, in some applications, the change of the grasped object weight [12]. When an exact object model is not available it can be approximated using geometric primitives [13] or learning methods can be applied to transfer a successful grasp of a known object to novel objects [14]. Uncertainty on the object shape has been modeled as constraints in the grasp planner [15], or as a noise managed using probabilistic techniques [16,17]. When the model of the object is completely unknown, a haptic exploration of the object surface can be performed prior to compute the grasp [18]. Other than the contact points, the execution of a grasp also requires the computation of proper grasping forces, which is another complex problem [19].

There are many quality indexes to evaluate the grasp quality [20,21]. One of the most used indexes is the measure of the largest perturbation wrench that the grasp can resist in any direction [22], but it does not consider the hand configuration. When the grasp can counterbalance a perturbation wrench in any direction, it is called a *force-closure* grasp (FC grasp) [23].

Tactile sensing systems based on different sensing techniques have been developed during the last decades in order to equip robots with tactile feedback [24,25]. Tactile feedback provides relevant information in many robotics applications [26]. In object manipulation, it reduces the uncertainty allowing, for instance, an improvement of the grasp stability and safety [27–29]. The tactile information obtained during the manipulation can also be used jointly with the hand kinematics to identify the model of the manipulated object [30], or jointly with visual feedback to improve the control performance [31].

Kinematics and control of multifingered hands manipulating an object with rolling contacts were already studied, but information about the mass, the center of mass and the geometry of the object is required [32]. On the other hand, different control strategies were proposed to deal with the manipulation of unknown objects, but tactile feedback is not always considered. A position-force control scheme was used to manipulate the object following a predefined trajectory [33], but it was evaluated only in simulation introducing noise on the sensor measurements to simulate a real environment. A torque controller was used to optimize the the applied grasping force over an object with smooth curvatures and a predefined shape [34], the approach can grasp objects with different shapes, but the experimental results were only performed in simulations without tactile sensors. A position-force controller was also used to slide the fingers on the object surface to explore and recognize it [35]. Another approach uses only a position control law to change the pose of the manipulated object [36], but it lacks of sensory feedback which is a hard limitation.

The manipulation space is the n -dimensional space defined by the values of all the finger joints, where a point represents a configuration of the hand and a curve represents a finger movement (i.e., a sequence of hand configurations). Then, doing a desired manipulation means following an appropriate curve in this space. However, computing a manipulation curve in advance may not be possible due to the unknown shape of the object, i.e., the manipulation constraints cannot be computed a priori and therefore planning a sequence of finger movements is not possible. In these conditions, manipulation must be a reactive procedure that determines on-line the proper hand movements. One straightforward way is the use of an exploration method [2] to search for hand configurations that improve a manipulation index, i.e., the fingers are moved following a predefined strategy and if the result improves the grasp (according to any quality index), a new step is done, otherwise the movement is drawn back and a new one is tested. In other words, it is like a blind search in the grasp space.

In this context, the main contributions of this work are: first, the proposal of a relationship between the finger joints and the manipulation indexes, i.e., the indexes are expressed as functions of the hand joint values, and second, a simple procedure to optimize the grasp of an unknown object by determining on-line the hand movements to manipulate the object following the gradient of these functions. As a result, with relatively simple geometrical reasoning and assumptions, an unknown object can be manipulated keeping the grasping forces in a desired range and preventing the object from falling despite uncertainty. It must be remarked that the expression “unknown object” means that the model of the object is not used at all in the manipulation procedure. Actually, as stated above, the shape of the object can be reconstructed using tactile and kinematics information during the manipulation [30]. These contributions make the approach presented in this work completely different from the approach presented in [2], where a blind search is performed to improve the grasp according to any index.

Tactile and kinematic data are inputs to the proposed manipulation process, which is a reactive procedure that controls locally the movements and contact forces to prevent the object from falling. The hand configuration is iteratively changed to manipulate the object optimizing three indexes associated with the three manipulation goals mentioned above, either individually or properly combined. Nevertheless, even when the computed movements should always improve the grasp quality, due to the unknown shape of the manipulated object and the different sources of noise and uncertainty, the actual grasp quality may eventually decrease in some manipulation steps.

The remaining of the paper is organized as follows. The proposed approach is detailed in Section 2. Section 3 introduces the three manipulation strategies to deal with each of the above mentioned manipulation goals. The experimental setup and results are presented in Section 4. Finally, some conclusions and future work are presented in Section 5.

2. Proposed Approach

2.1. Problem Statement, Approach Overview and Assumptions

The problem addressed in this work is the manipulation of unknown objects pursuing one or more of the manipulation goals mentioned in Section 1, i.e., optimizing the grasp from the point of view of the hand, the object, and the hand-object relationship. We remark again that “unknown object” means that the model of the object is not used at all in the manipulation procedure.

The aim of the proposed approach is, after performing a FC grasp of an object, to iteratively determine the movements (sequences of hand configurations) to improve a manipulation index according to the mentioned goals. The initial grasp could be non-optimal due to several reasons (e.g., accessibility or position uncertainty), but in any case the planning and execution of the initial grasp is outside the scope of this work.

Once the pursued goal is defined, an iterative procedure is started and in each iteration the only inputs are the tactile feedback and the kinematic configuration of the hand. The computation of the finger movements is done following a specific manipulation strategy for each of the mentioned goals (but they can be merged as described in Section 3.4), and a specific index to be minimized is defined to measure the quality of the manipulation actions. The iterative procedure ends when the corresponding index reaches a known minimum value, the index has not decreased after a predefined number of iterations, or the grasp configuration is getting close to the security limits imposed by the friction constraints.

The following assumptions are considered in this work:

- The robotic hand has tactile sensors to obtain information about the contacts with the manipulated object, and no other feedback source is available, as, for instance, visual information.
- Two fingers of the hand are used for the manipulation. These fingers perform a grasp comparable with a human grasp using the thumb and index fingers with the fingertips movements lying on

plane [37]. This type of grasp limits the movement of the object to a plane but it allows different actions in every-day and industrial tasks, like, for instance, matching the orientation of two pieces to be assembled or inspecting an object [38,39].

- The manipulated objects are rigid bodies and their shape is unknown. The approach could work also for soft objects, there is not any specific constraint for it, but we did not determine in this work any limit for the acceptable softness.
- The friction coefficient is not identified during the manipulation. It is assumed to be above a minimum security value which can be roughly determined considering the object material and the rubber surface of the fingertips. In the experimentation we compute the movements using the minimum value of the friction coefficient between the material of the fingertips and the used objects, i.e., a value below the real friction coefficient.
- The finger joints have a low-level position control to make them reach the commanded positions, which is the most frequent case in a commercial hand with a closed controller. No force control is required at the level of the hand controller. The proposed approach uses the tactile measurements to generate commanded positions, thus it is actually acting as an implicit upper level force control loop.

2.2. Grasp Modeling

Figure 1 shows the geometric model of a two-finger grasp. A finger f_i , $i \in \{1, 2\}$, is a kinematic serial chain with n_i degrees of freedom (DOF) and n_i links with length l_{ij} , $j \in \{1, \dots, n_i\}$. A joint angle q_{ij} relates the position of each link to the previous one. The configuration of the finger f_i is given by its joints angles as $\mathbf{q}_i = \{q_{i1}, \dots, q_{in_i}\}$. A hand configuration is given by the concatenation of the configurations of the two used fingers as $\mathbf{Q} = \{\mathbf{q}_1, \mathbf{q}_2\}$. Each finger link has a reference frame Σ_{ij} fixed at its base, and the absolute reference frame Σ_O is located at the base of the finger f_1 .

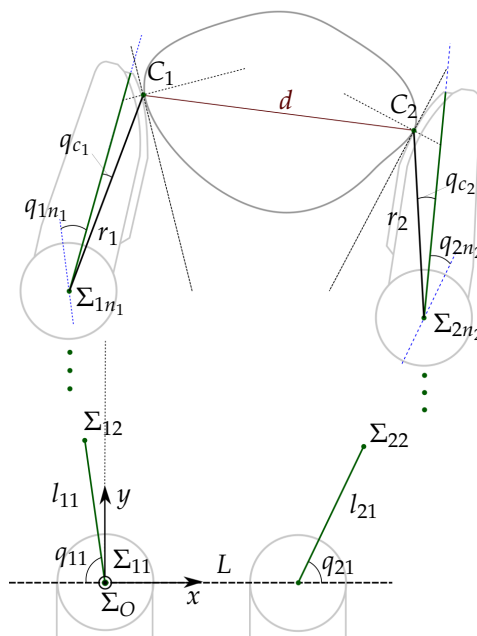


Figure 1. Geometric model of a two-finger grasp.

In general, the contact between a fingertip and the object produces contact regions on the sensor pad. In this work the contact between each fingertip and the object is modeled using the punctual contact model [40]. Note that this is a consideration for the grasp modeling, since the contact on a fingertip actually may take place over a contact region which may also be composed by several

disjoint subregions. For the contact model, in this work the barycenter of the actual contact region (either a single one or a set of disjoint subregions) is considered to be the current contact point. Besides, the summation of the forces sensed at each texel in the actual contact region is considered to be the current contact force applied by the finger at the equivalent punctual contact [41].

Let C_i be the position of the contact point on finger f_i with respect to Σ_O . C_i is computed using direct kinematics of the fingers and the information provided by the tactile sensor. A virtual link is used to include the contact point information into the hand kinematics (see Figure 1). This virtual link adds a non-controllable extra DOF to each finger, which is defined by the angle q_{c_i} or by the length r_i of the segment between the origin $O_{\Sigma_{in_i}}$ of the reference frame Σ_{in_i} , and the contact point C_i . Then, the Euclidean distance d between the contact points C_1 and C_2 is given by

$$d(C_1, C_2) = \|\overline{C_1 C_2}\| = \sqrt{(C_{1x} - C_{2x})^2 + (C_{1y} - C_{2y})^2} \quad (1)$$

2.3. Main Manipulation Algorithm

Algorithm 1 shows the main manipulation procedure, which is general and valid for any manipulation strategy. As inputs, the user selects the desired contact force F_d and the manipulation strategy (MS) to pursue one of the three manipulation goals mentioned in Section 1 or a combination of them. The manipulation process starts with a blind grasp of the object, closing the fingers along a predefined path until F_d is reached and the object has been securely grasped (lines 2 to 4). Then, the object is manipulated with an iterative procedure following the selected manipulation strategy. Each iteration k involves the following parts:

1. Computation of the relevant variables of the current grasp state (lines 6 to 7). C_{1_k} and C_{2_k} are obtained using the hand kinematics and the tactile information, and the magnitude of the grasping force F_k is obtained as the average of the contact forces F_{1_k} and F_{2_k} measured on each fingertip. Although F_{1_k} and F_{2_k} should have the same magnitude and opposite direction, the use of the average of both measured contact forces minimizes potential measurement errors, thus

$$F_k = \frac{F_{1_k} + F_{2_k}}{2} \quad (2)$$

2. Computation of two virtual contact points $C_{1_{k+1}}^*$ and $C_{2_{k+1}}^*$ (line 8). These points are such that the movements of the fingers to make them be the new contact points changes the grasp towards the selected goal. The computation of $C_{1_{k+1}}^*$ and $C_{2_{k+1}}^*$ from C_{1_k} and C_{2_k} according to each manipulation strategy MS are detailed in the next section.
3. Computation of the new hand configuration $Q_{k+1} = \{q_{1_{k+1}}, q_{2_{k+1}}\}$ (lines 10 to 12). Since the shape of the object is unknown, any movement of the fingers may alter the contact force F_k allowing potential damage of the object or the hand if it increases or allowing a potential fall of the object if it decreases. In order to reduce the error $e = F_k - F_d$, the distance d_k is adjusted in each iteration as

$$d_{k+1} = d_k + \Delta d \quad (3)$$

with

$$\Delta d = \begin{cases} f_1(e) & \text{if } e \leq 0 \\ f_2(e) & \text{if } e > 0 \end{cases} \quad (4)$$

where $f_1(e)$ and $f_2(e)$ are user defined functions. In this work, we use $f_1(e) = 2\lambda(e + e^2)$ and $f_2(e) = \lambda e$, with λ being a predefined constant. The reason for this is that a potential fall of the object ($F_k \rightarrow 0$) is considered more critical than a potential application of large grasping forces ($F_k \gg F_d$), and therefore $f_1(e)$ has larger gain, specially for large $|e|$.

Algorithm 1: Tactile Manipulation

```

Inputs :  $F_d, MS$ 
1  $k \leftarrow 0, F_k \leftarrow 0, stop \leftarrow false$ 
  // Execution of the initial blind grasp
2 while  $F_k < F_d$  do
3   | Close the fingers
4   | Compute  $F_k$  using Equation (2)
  // Manipulation procedure
5 while  $stop \neq true$  do
  // Obtainment of the current state of the grasp
6   Compute  $C_{1k}$  and  $C_{2k}$  using Forward Kinematics
7   Compute  $F_k$  using Equation (2)
  // Application of the manipulation strategy
8   Compute the virtual contact points  $C_{i_{k+1}}^*$  according to MS
9   Compute the quality index associated to MS
  // Computation of the new hand configuration
10  Compute  $d_{k+1}$  using Equation (3)
11  Compute  $C_{i_{k+1}}$  using Equation (5)
12  Compute  $Q_{k+1}$  from  $C_{i_{k+1}}$  using Inverse Kinematics
  // Verification of termination conditions
13  if Termination conditions are not satisfied then
  | // Finger movement
14  | Move  $f_i$  through  $Q_{k+1}$ 
15  |  $k \leftarrow k + 1$ 
16  else
17  |  $stop \leftarrow true$ 

```

Now, $C_{1_{k+1}}^*$ and $C_{2_{k+1}}^*$ are adjusted along the line they define to obtain the actual target contact points $C_{1_{k+1}}$ and $C_{2_{k+1}}$ at a distance d_{k+1} ,

$$C_{i_{k+1}} = R_{k+1} + \frac{d_{k+1}}{2} \delta_{i_{k+1}}, \quad i \in \{1, 2\} \quad (5)$$

where R_{k+1} is the central point between $C_{1_{k+1}}^*$ and $C_{2_{k+1}}^*$ and $\delta_{i_{k+1}}$ is the unitary vector from R_{k+1} to $C_{i_{k+1}}^*$ (see Figure 2).

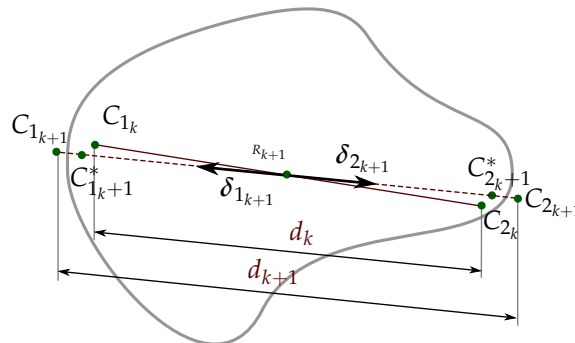


Figure 2. Example of the computation of $C_{i_{k+1}}$ using $C_{i_{k+1}}^*$, adjusting the distance d_k to d_{k+1} when the contact force F_k is larger than F_{max} .

Finally, using the inverse kinematics of the fingers, from the points $C_{1_{k+1}}$ and $C_{2_{k+1}}$ it is possible to obtain the corresponding hand configuration $Q_{k+1} = \{q_{1_{k+1}}, q_{2_{k+1}}\}$.

Figure 3 illustrates the relationship between the measured variables, the role played by the manipulation strategy in the computation of the auxiliary variables $C_{i_{k+1}}^*$, and the variables involved in the final adjustment to obtain the new hand configuration (with independence of the manipulation strategy).

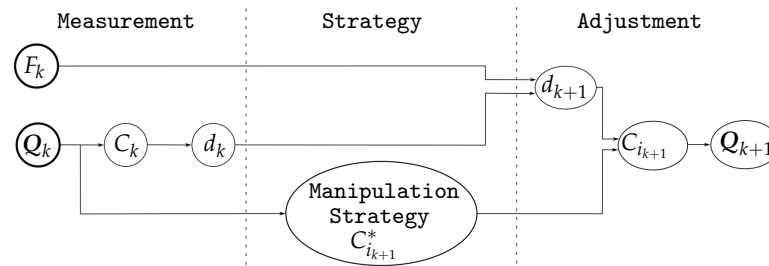


Figure 3. Relation between the measured variables, the role of the manipulation strategy, and the final adjustment to obtain the new hand configuration.

4. Termination conditions (line 13). The iterative manipulation procedure is applied until any of the following four stop conditions is activated, two of them associated with the quality index and the other two with the motion constraints:
 - The quality index reaches the optimal value.
 - The current optimal value of the quality index is not improved during a predetermined number of iterations. Note that the index may not be improved monotonically, it could become worse or oscillate alternating small improvements and worsening.
 - The expected grasp at the computed contact points does not satisfy the friction constraints.
 - The computed contact points do not belong to the workspace of the fingers. This condition is activated when the computed target contact points $C_{1_{k+1}}$ and $C_{2_{k+1}}$ are not reachable by the fingers, i.e., $Q_{k+1} = \{q_{1_{k+1}}, q_{2_{k+1}}\}$ does not lie within the hand workspace.
5. Finger movements (line 14). When none of the termination conditions is activated, the hand is moved towards Q_{k+1} to make the fingers reach the desired target contact points $C_{1_{k+1}}$ and $C_{2_{k+1}}$. After the finger movements a new manipulation iteration begins.

3. Manipulation Strategies

This section presents the manipulation strategies to optimize the hand configuration, the grasp quality and the object orientation, or a combination of them, according to a desired goal using only information from the current hand configuration and from the tactile sensors. The following subsections introduce the index to be optimized and the procedure to generate the two virtual contact points $C_{1_{k+1}}^*$ and $C_{2_{k+1}}^*$ for each manipulation strategy and for a combination of them.

3.1. Optimizing the Hand Configuration

3.1.1. Index to be Optimized

The optimization of the hand configuration implies that the fingers must try to reach specific positions while preventing the fall of the object. These positions are generally defined by the middle-range positions of the joints, but it could be also arbitrarily defined by the user according to the particular features of the used hand (in the middle-range positions the joints are far away from their mechanical limits, thus there is a potential wider range of movements).

Let $q_{0_{ij}}$ be the predefined desired specific position of the j -th joint of the finger i , then $Q_0 = \{q_{0_{ij}}, i \in \{1, 2\}, j \in \{1, n_i\}\}$ is the desired specific configuration of the hand. Then, the goodness of the hand configuration is indicated by a quality index I_{hc} computed according to the current joint values q_{ij} as

$$I_{hc} = \sum_{i=1}^2 \sum_{j=1}^{n_i} \left(\frac{q_{ij} - q_{0_{ij}}}{q_{\max_{ij}} - q_{\min_{ij}}} \right)^2 \quad (6)$$

where $q_{\max_{ij}}$ and $q_{\min_{ij}}$ are the maximum and minimum limits of the j -th joint of the finger i , respectively. The hand configuration is improved by minimizing I_{hc} , which favors the hand configurations with the joints as close as possible to the desired specific positions [42].

3.1.2. Optimization Strategy

In this case, the goal configuration of the hand is known with independence of the object shape, thus it is trivial to move the hand towards it, the key point is to do it allowing an adequate adjustment of the distance d_k between the contact points in each iteration to prevent the object from falling. Then, the hand configuration is updated in each iteration as

$$Q_{k+1}^* = Q_k + \Delta Q \quad (7)$$

where

$$\Delta Q = \eta(Q_0 - Q_k) \quad (8)$$

is a small enough vector pointing from the current configuration $Q_k = \{q_{1k}, q_{2k}\}$ to Q_0 , i.e., η must be chosen to properly fix the advance of the hand configuration in each iteration. As a practical approach, when the angles are measured in degrees, $\Delta Q \leq 1$ was found to work well, this is achieved with

$$\eta = \frac{\tanh(\|Q_0 - Q_k\|)}{\|Q_0 - Q_k\|} \quad (9)$$

where \tanh is used to bound η when the current configuration of the hand Q_k is far from Q_0 . From Equations (8) and (9) results

$$\Delta Q = \frac{\tanh(\|Q_0 - Q_k\|)}{\|Q_0 - Q_k\|} (Q_0 - Q_k) \quad (10)$$

Finally, from Q_{k+1}^* it is straightforward to obtain the virtual contact points $C_{1_{k+1}}^*$ and $C_{2_{k+1}}^*$ using the direct kinematics of the hand.

Figure 4 summarizes the relation between the variables involved in the computation of $C_{1_{k+1}}^*$ and $C_{2_{k+1}}^*$ for the optimization of the hand configuration (according to the general diagram shown in Figure 3).

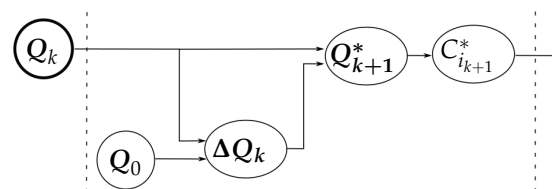


Figure 4. Variables involved in the optimization of the hand configuration.

3.2. Optimizing the Grasp Quality

3.2.1. Index to be Optimized

The optimization of the grasp quality implies that the fingers must manipulate the object increasing the security margin of the force-closure grasp given by the angles $\beta_i, i \in \{1, 2\}$ (see Figure 5). i.e., the segment connecting both contact points must lie far from the boundary of the friction cones. Then, the grasp quality is measured using a quality index I_{gq} based on the angles β_i as

$$I_{gq} = \frac{1}{2} \sum_{i=1}^2 |\beta_i| \quad (11)$$

Thus, the grasp quality is improved by minimizing I_{gq} .

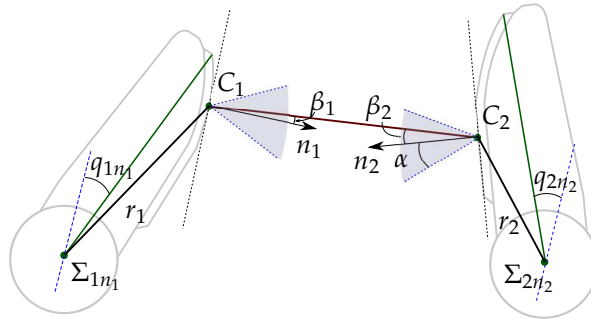


Figure 5. Fingertips and angles used to compute the friction constraints.

3.2.2. Optimization Strategy

Using basic geometry and the information obtained from the tactile sensors and the finger kinematics, the angles β_i can be computed as functions of the current contact points C_i , the origin $O_{\Sigma_{in_i}}$ of the reference frame Σ_{in_i} , and the length r_i and the joint angle q_{c_i} of the virtual link at the fingertips (all the variables are computed for the iteration k , thus, to improve legibility, subindex k have been removed),

$$\beta_1 = \arccos \left(\frac{-|O_{\Sigma_{in_1}} C_2|^2 + r_1^2 + |C_1 C_2|^2}{2r_1 |C_1 C_2|} \right) + q_{c_1} - \pi \quad (12)$$

$$\beta_2 = \arccos \left(\frac{-|O_{\Sigma_{in_2}} C_1|^2 + r_2^2 + |C_1 C_2|^2}{2r_2 |C_1 C_2|} \right) + q_{c_2} - \pi \quad (13)$$

The gradient of $\beta_i(Q_k)$ at the current configuration of the hand, $\nabla \beta_i(Q_k)$, is used to compute the next virtual configuration of the hand Q_{k+1}^* as

$$Q_{k+1}^* = Q_k + \Delta Q \quad (14)$$

where ΔQ is now given by

$$\Delta Q = \frac{1}{2} \tanh(\beta_1) \frac{\nabla \beta_1}{\|\nabla \beta_1\|} + \frac{1}{2} \tanh(\beta_2) \frac{\nabla \beta_2}{\|\nabla \beta_2\|} \quad (15)$$

Finally, as in the previous strategy, from Q_{k+1}^* it is straightforward to obtain the virtual contact points $C_{i_{k+1}}^*$ and $C_{i_{k+1}}^*$ using the direct kinematics of the hand.

Figure 6 summarizes the relation between the variables involved in the computation of $C_{1_{k+1}}^*$ and $C_{2_{k+1}}^*$ for the optimization of the grasp quality (according to the general diagram shown in Figure 3).

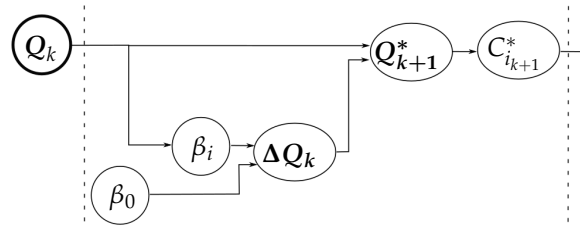


Figure 6. Variables involved in the optimization of the grasp quality.

3.3. Optimizing the Object Orientation

3.3.1. Index to be Optimized

The optimization of the object orientation implies that the fingers must rotate the object towards a desired goal orientation. The orientation of the object in the initial blind grasp is considered as $\gamma_0 = 0$, and therefore the desired orientation of the object γ_d is relative to it. Then, the manipulation strategy must reduce the difference between γ_d and the current object orientation γ_k . The quality index could be just the orientation error $|\gamma_d - \gamma_k|$, but in order to constrain it to the range $[0, 1]$ it is normalized dividing by $\gamma_i - \gamma_d$, γ_i being the current orientation at the time γ_d is given, i.e.,

$$I_{oe} = \left| \frac{\gamma_d - \gamma_k}{\gamma_d - \gamma_i} \right| \quad (16)$$

3.3.2. Optimization Strategy

The orientation of the object γ_k can be computed using basic geometry and the information obtained from the tactile sensors and the finger kinematics, no other external feedback is considered (like, for instance, a vision system) although it could exist at a higher level (for instance to determine γ_d , but this is outside of the scope of this work). For fingertips with circular shape, the current object orientation γ_k is given by [43]

$$\gamma_k = \frac{2R + d_k}{d_k}(\theta_0 - \theta) + \frac{R}{d_k} \sum_{j=1}^{n_1} (q_{1j\gamma_0} - q_{1jk}) - \sum_{j=1}^{n_2} (q_{2j\gamma_0} - q_{2jk}) \quad (17)$$

being

- θ the average of the two angles between an arbitrary reference axis attached to the object and the directions normal to each fingertip at the corresponding contact point,
- θ_0 the value of θ at the initial grasp (i.e., for γ_0),
- q_{ijk} the current value of the ij -th joint (i.e., joint $j = 1, \dots, n_i$ of finger $i = 1, 2$),
- $q_{ij\gamma_0}$ the value of the ij -th joint at the initial grasp (i.e., for γ_0),
- d_k the distance between the contact points, and
- R the radius of the fingertip.

The first term in Equation (17) has a factor that depends on the variation of θ , then, since θ does not change significantly during the manipulation (i.e., $\theta \approx \theta_0$) the first term can be neglected. Thus, γ_k can be approximated by

$$\gamma_k \approx \frac{R}{d_k} \sum_{j=1}^{n_1} (q_{1j\gamma_0} - q_{1jk}) - \sum_{j=1}^{n_2} (q_{2j\gamma_0} - q_{2jk}) \quad (18)$$

Since the finger movements are small and γ_k is recomputed in each iteration, this approximation is accurate enough for the manipulation goal.

Now, the virtual contact points C_{1k+1}^* and C_{2k+1}^* are computed considering that the fingers are moved to produce the displacement of the contact points on the sensor pad along a circular path given by (see Figure 7):

$$C_{1k+1x}^* = R_{kx} - (d_k/2) \cos(\gamma_{k+1}) \tag{19}$$

$$C_{1k+1y}^* = R_{ky} - (d_k/2) \sin(\gamma_{k+1}) \tag{20}$$

$$C_{2k+1x}^* = R_{kx} + (d_k/2) \cos(\gamma_{k+1}) \tag{21}$$

$$C_{2k+1y}^* = R_{ky} + (d_k/2) \sin(\gamma_{k+1}) \tag{22}$$

i.e., the new virtual positions are points on a circumference with diameter d_k centered at the middle point, R_k , between the points C_{1k} and C_{2k} , and

$$\gamma_{k+1} = \gamma_k + \tanh(\gamma_k)\Delta\gamma \tag{23}$$

$\Delta\gamma$ is chosen empirically and small enough to assure small movements of the object in each manipulation step.

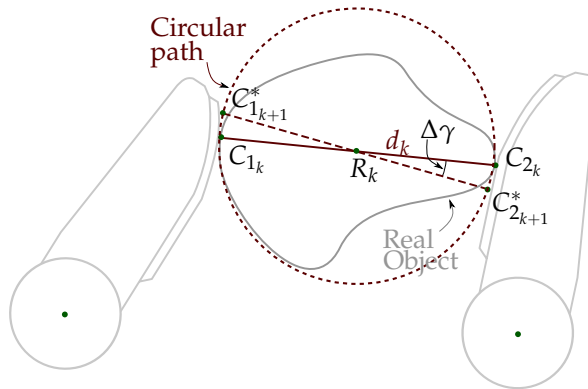


Figure 7. Movements used for the optimization of the object orientation. C_{1k+1} and C_{2k+1} are computed over a circular path with diameter d_k centered at R_k .

Note that in this case it was not necessary to compute Q_{k+1} as an intermediate step to determine the virtual contact points $C_{i_{k+1}}^*$. Instead, now Q_{k+1} can be deduced from $C_{i_{k+1}}^*$ applying inverse kinematic. This is relevant since the direction of $\Delta Q = Q_{k+1} - Q_k$ is necessary to combine different manipulation strategies, as will be shown in Section 3.4.

Figure 8 summarizes the relation between the variables involved in the computation of C_{1k+1}^* and C_{2k+1}^* for the optimization of the object orientation (according to the general diagram shown in Figure 3).

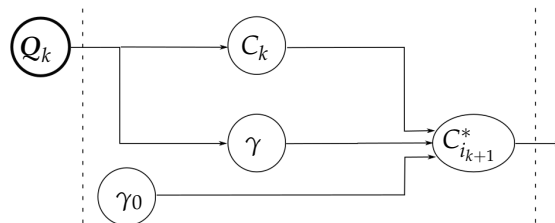


Figure 8. Variables involved in the optimization of the object orientation.

3.4. Combining Manipulation Strategies

3.4.1. Index to be Optimized

The approach allows the combination of two or more manipulation strategies, for this purpose a combined quality index I_{cq} is computed as a lineal combination of the quality indexes associated to the combined manipulation strategies, i.e.,

$$I_{cq} = \sum_j \omega_j I_j \quad (24)$$

where $\omega_j > 0$ are weighting coefficients.

3.4.2. Optimization Strategy

When two or more manipulation strategies are combined, the target configuration of the hand Q_{k+1} is computed as the current hand configuration plus a lineal combination of the incremental movements ΔQ_j obtained by each manipulation strategy j individually, i.e.,

$$Q_{k+1}^* = Q_k + \sum_j \omega_j \Delta Q_j \quad (25)$$

with $\omega_j > 0$ satisfying $\sum_j \omega_j = 1$ to avoid unexpected large movements. The coefficients ω_j can be arbitrarily adjusted to give different weights to each combined strategy. It must be remarked that the final movement determined to optimize the combined index does not imply the individual optimization of all the involved individual indexes.

Then, from Q_{k+1}^* it is straightforward to obtain the virtual contact points C_{1k+1}^* and C_{2k+1}^* using the direct kinematics of the hand.

4. Experimental Validation

The proposed approach has been fully implemented using C++. The system setup and some examples of experimental results are presented below to illustrate the performance of the approach.

4.1. System Setup

The Schunk Dexterous Hand (SDH2) shown in Figure 9a was used for the experimental validation. This is a three-finger hand, each finger has two DOF and another one allows the rotation of two fingers around their bases to work opposite to each other, making a total of seven DOF. The SDH2 has tactile sensors on the surface of the proximal and distal phalanges. A detailed description of the hand kinematics is presented in [44]. In this work, only the fingertips of the two fingers working opposed to each other are used for the manipulation. The sensor surface on the fingertips is composed of a planar part with length 16 mm and a curve part with radius 60 mm (Figure 9b). The planar part of the sensor pad includes the rows of texels 1 to 5, and the curved part the rows of texels 6 to 13; the wide of the sensor is 6 texels in the lower part and 4 texels in the upper part, making a total of 68 sensitive texels (Figure 10). Each texel of the sensor pads returns a value from 0, when no pressure is applied, to 4095, for a maximum measurable normal force per texel of 3 N. As stated in Section 2.2, we consider the barycenter of the contact region as the current contact point between the object and the fingertip and the summation of the forces over all the texels in the contact region as the current contact force [41] (see Figure 10). It must be noted that when the contact is produced only on one or two texels the measured force is limited to up to 3 or 6 N respectively and these cases must be specially considered to avoid pushing the fingers trying to get larger forces. Besides, since the tactile sensors do not provide tangential components of the grasping forces, in the experiments the actual contact force could be larger than the measured one, which is not a significant problem, unless extremely fragile objects are manipulated and the normal forces are quite close to the maximal tolerated forces.

There are proposals of tactile sensing devices that allow the measurement of the real applied forces [45]. Nevertheless, since the proposed approach also considers the angles β_i between the normal directions at the contact points and the force direction (defined by the contact points), the explicit measurement of the tangential force component is not necessary for the computation of the grasp security margin.

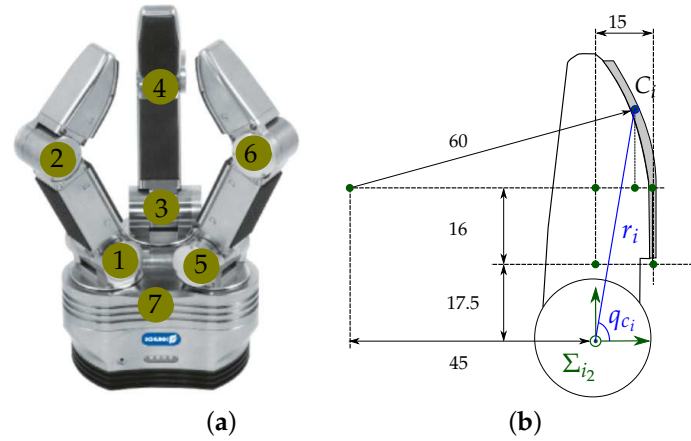


Figure 9. (a) Schunk Dexterous Hand (SDH2) with joints labels; (b) lateral view of the fingertip with the sensor pad (distances are in millimeters).

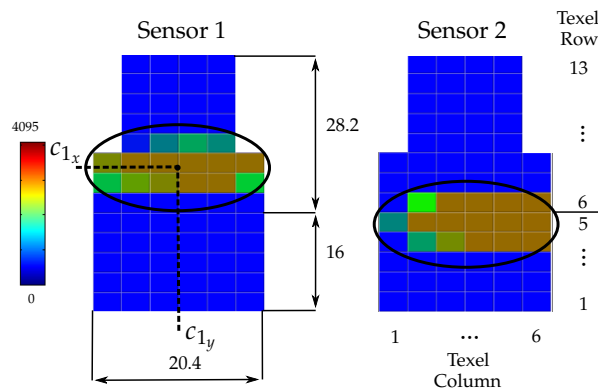


Figure 10. Graphical representation of tactile measurements highlighting with ellipses the contact region on each sensor pad. The bar in the left indicates the scale of colors corresponding to the force values returned by each texel, the range of returned values from 0 to 4095 corresponds to a range of forces from 0 to 3 N. The five lower rows of texels correspond to the planar part of the sensor. All the lengths are in millimeters. (see also Figure 9c).

4.2. Experimental Results

In the following illustrative examples the fingers are blindly closed around an unknown object until the measured grasping force reaches an arbitrary desired value $F_d = 5$ N. This force value was chosen considering the range of the tactile sensors, the forces the hand can apply and that the manipulated objects were hard rigid bodies. The objects used for the experiments were selected looking for different object shapes (with small and large curvatures) and different object boundaries (smooth and irregular), so the performance of the proposed approach can be illustrated under different conditions. The initial position of the object varies in each execution of the experiments and therefore the initial grasp configuration and the initial contact points are unknown a priori by the system. The friction coefficient considered in the calculations was $\mu = 0.4$ (friction cone angle of only $\alpha = 21.8$ degrees), which is below the expected real physical value. The constant λ to adjust the

distance between the contact points according to Equation (4) was set to $\lambda = 0.25$ mm. Videos of experimental executions can be found in <http://goo.gl/ivFd0q>.

In Examples 1 to 4 (Figures 11–14, respectively) four different objects are manipulated improving the three quality indexes sequentially, first the manipulation optimizes I_{gq} , then I_{hc} and finally I_{oe} . When I_{gq} is improved, the angles β_i are minimized according to the expected behavior of the manipulation strategy. For the improvement of I_{hc} , $Q_0 = \{-45, 45, -45, 45\}$ is considered as the desired hand configuration. Finally, for the improvement of I_{oe} , the desired goal is an object rotation of 5 degrees clockwise. On the sub-figures showing charting results, a vertical dotted line is depicted to highlight the iterations when the optimization index changes. Particular details of each experiment are given in the caption of each figure.

In Example 5 (Figure 15) the object was successively rotated clockwise and counterclockwise with desired orientations γ_d set to 5, -5 , 10, -10 , and 15 degrees. The change of setpoint was manually done once the system has activated a termination condition for the current setpoint. In the first four cases the termination condition was the arrival of I_{oe} to the expected value according to the system internal measurements, i.e., $\gamma_k \approx \gamma_d$ (see Figure 15c), and in the last case the manipulation ended because the expected next value of the angle β_1 exceeded the friction cone limit before arriving to $\gamma_d = 15$ degrees (see the evolution of β_1 in Figure 15f), meaning that there was a risk of sliding and the object could flip away from the hand. The real orientations of the object when the terminal conditions were activated, measured by an external vision system, are given in Figure 15c in parenthesis below the corresponding values obtained from internal measurements. $\Delta\gamma$ was set to 0.25 degrees.

In Example 6 (Figure 16) two manipulation strategies were combined, optimizing the hand configuration and the grasp quality simultaneously. The strategies were combined using $\omega_1 = \omega_2 = 0.5$ in Equations (24) and (25), i.e., $I_{cq} = 0.5I_{hc} + 0.5I_{gq}$. In this example β_i tends to zero according to the optimization of the grasp quality while the joints tend to their desired specific positions. The manipulation ended after 2.85 s and 38 iterations because I_{cq} did not improve the current optimal value during 10 iterations. Note that the optimization of I_{cq} does not imply the optimization of I_{hc} and I_{gq} .

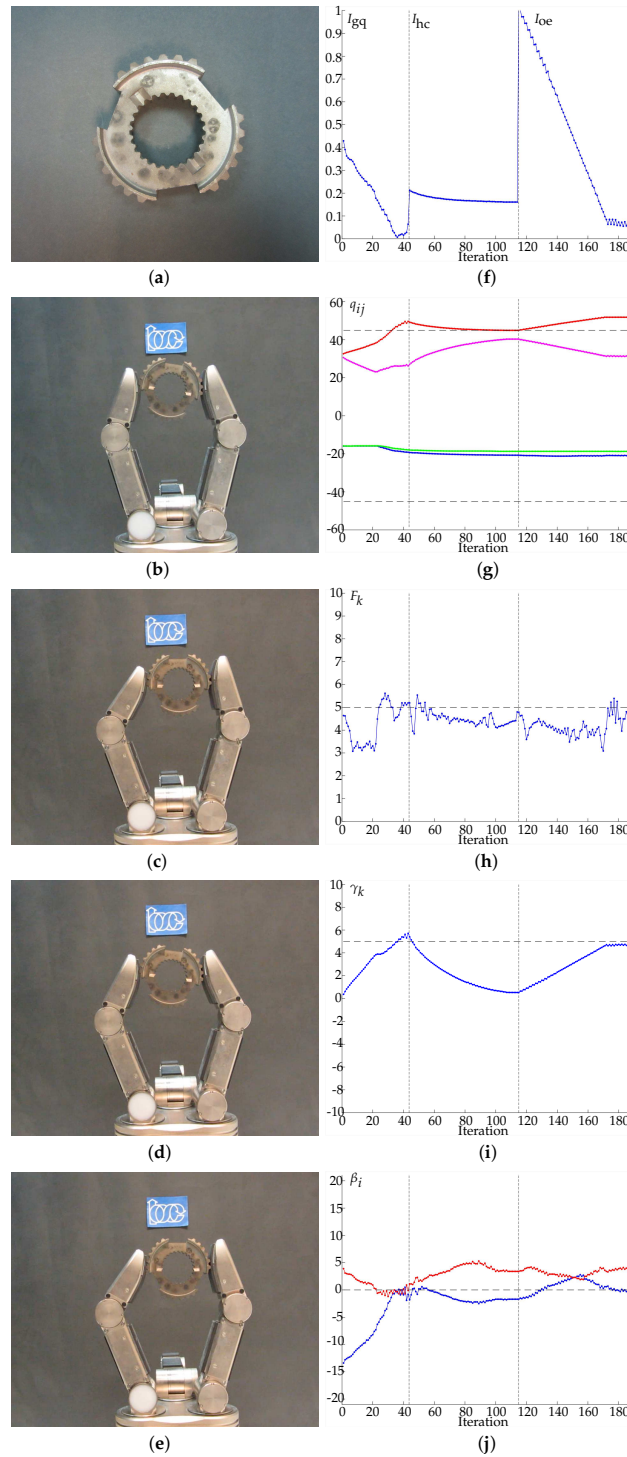


Figure 11. Example 1. (a) Manipulated object. (b) Initial grasp. (c) Hand configuration after optimizing I_{gq} . (d) Hand configuration after optimizing I_{hc} . (e) Hand configuration after optimizing I_{oe} . (f) Evolution of the quality indexes. The manipulations improving I_{gq} , I_{hc} and I_{oe} ended after 3.864 s and 43 iterations, 4.486 s and 70 iterations and 9.083 s and 73 iterations, respectively. (g) Evolution of the joints values in degrees, q_{11} in blue, q_{12} in red, q_{21} in green, q_{22} in magenta. (h) Average force F_k in Newtons, the dashed line indicates F_d . (i) Evolution of the object orientation in degrees. (j) Angles β_i in degrees, β_1 in blue and β_2 in red (the dashed line indicates the optimal value of β_i). Note that the non-smooth and toothed surface of the manipulated object produces more than one contact region on each fingertip without generating any manipulation problem.

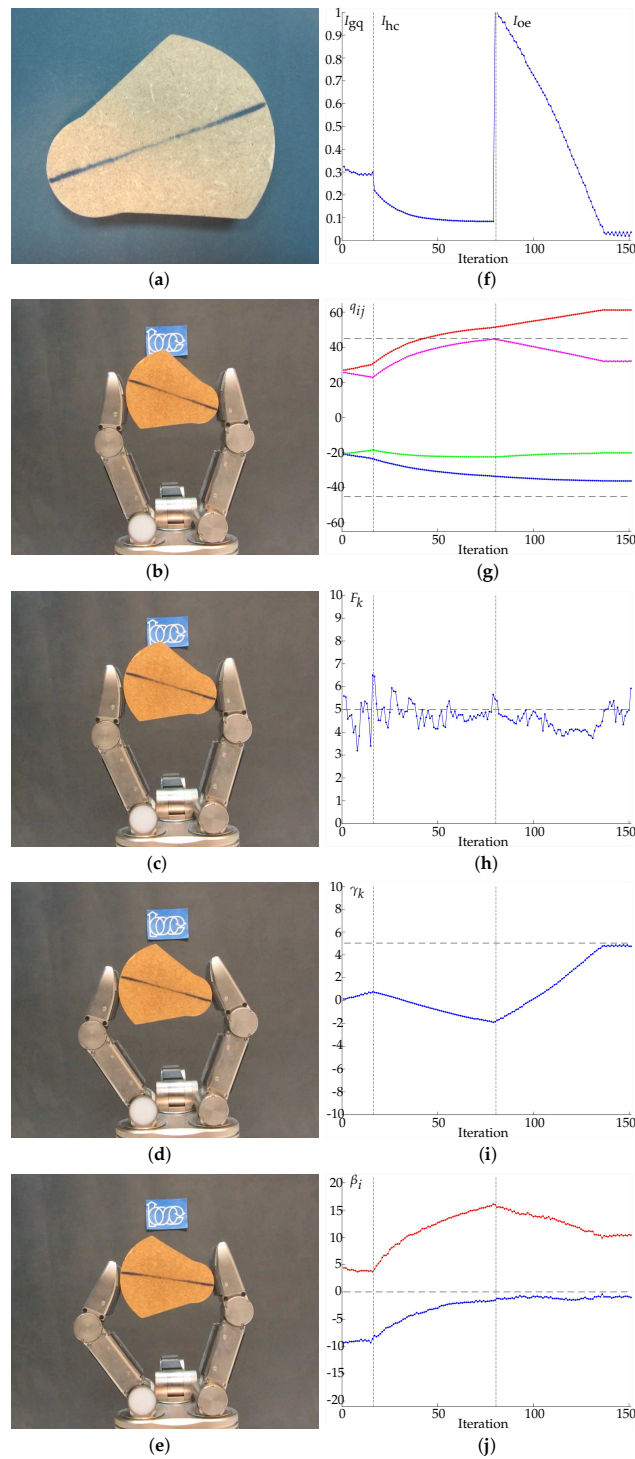


Figure 12. Example 2. (a) Manipulated object. (b) Initial grasp. (c) Hand configuration after optimizing I_{gq} . (d) Hand configuration after optimizing I_{hc} . (e) Hand configuration after optimizing I_{oe} . (f) Evolution of the quality indexes. The manipulations improving I_{gq} , I_{hc} and I_{oe} ended after 1.171 s and 16 iterations, 4.687 s and 62 iterations and 9.709 s and 71 iterations, respectively. (g) Evolution of the joints values in degrees, q_{11} in blue, q_{12} in red, q_{21} in green, q_{22} in magenta. (h) Average force F_k in Newtons, the dashed line indicates F_d . (i) Evolution of the object orientation in degrees. (j) Angles β_i in degrees, β_1 in blue and β_2 in red (the dashed line indicates the optimal value of β_i).

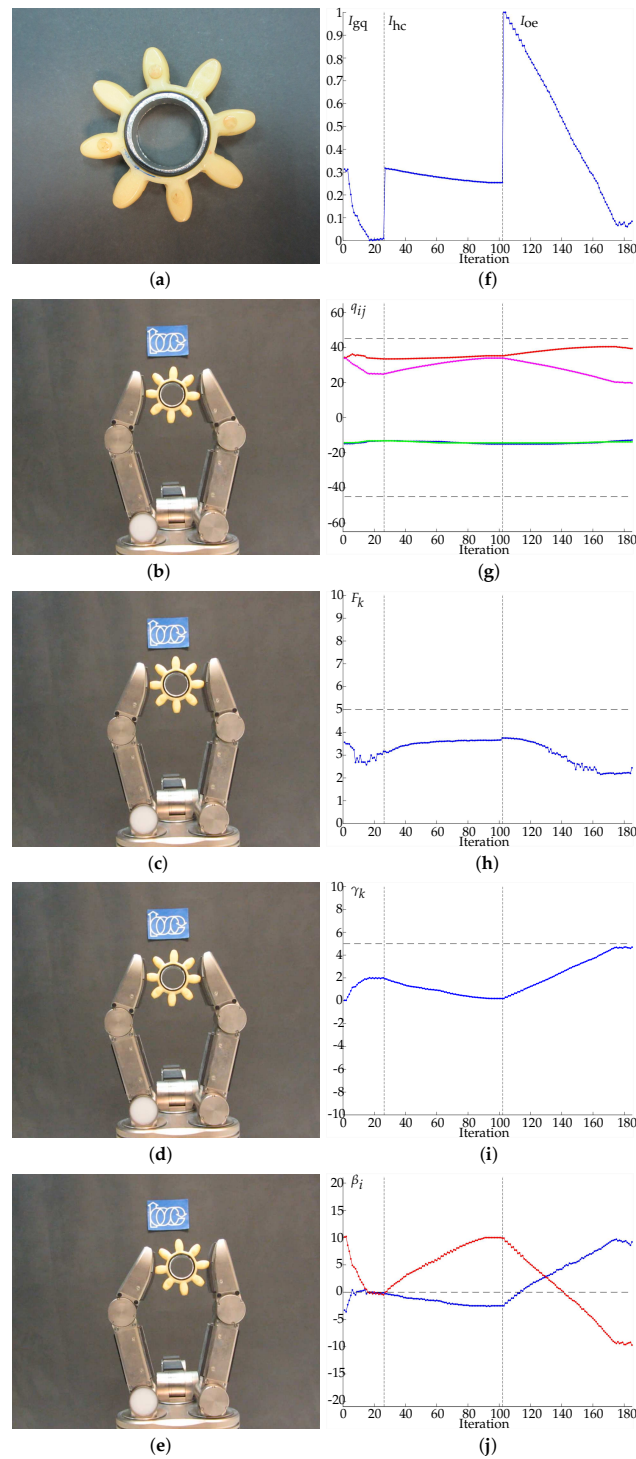


Figure 13. Example 3. (a) Manipulated object. (b) Initial grasp. (c) Hand configuration after optimizing I_{gq} . (d) Hand configuration after optimizing I_{hc} . (e) Hand configuration after optimizing I_{oe} . (f) Evolution of the quality indexes. The manipulations improving I_{gq} , I_{hc} and I_{oe} ended after 2.439 s and 26 iterations, 4.627 s and 75 iterations and 8.779 s and 82 iterations, respectively. (g) Evolution of the joints values in degrees, q_{11} in blue, q_{12} in red, q_{21} in green, q_{22} in magenta. (h) Average force F_k in Newtons, the dashed line indicates F_d . (i) Evolution of the object orientation in degrees. (j) Angles β_i in degrees, β_1 in blue and β_2 in red (the dashed line indicates the optimal value of β_i). Note that, due to the shape of the manipulated object, the contact is produced on a limited region of the sensor and therefore the force F_k cannot reach the desired force F_d .

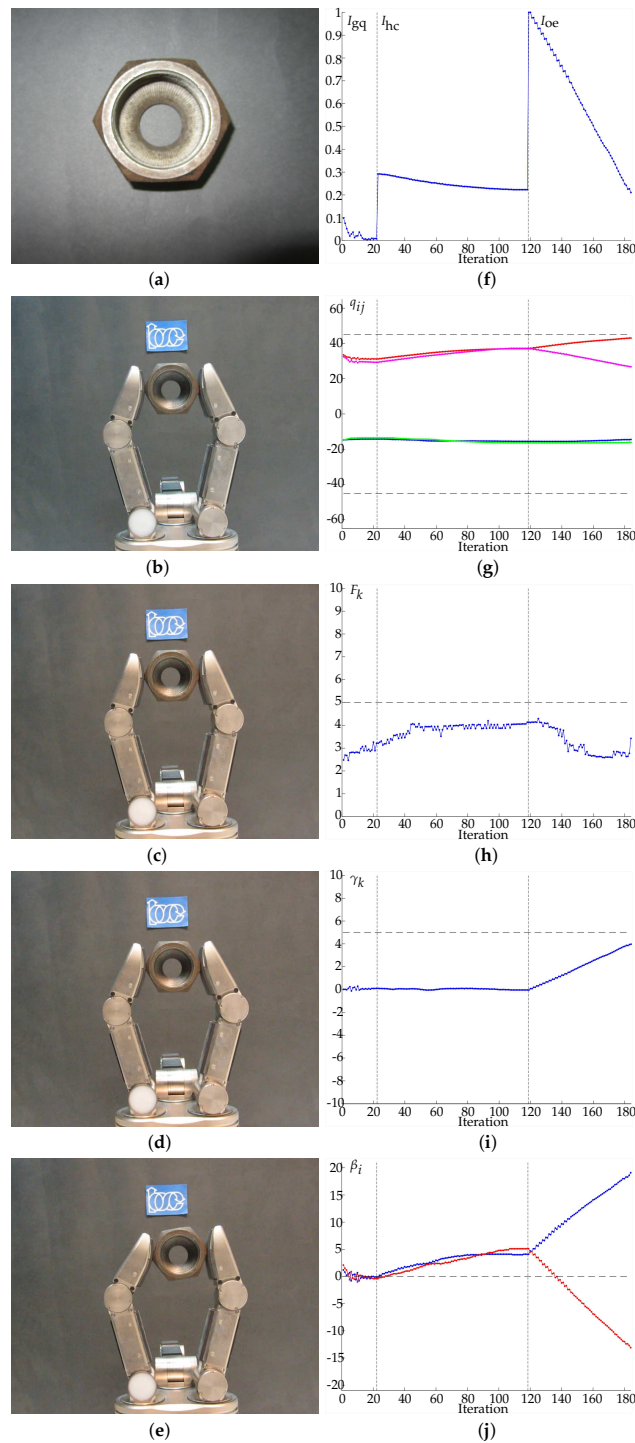


Figure 14. Example 4. (a) Manipulated object. (b) Initial grasp. (c) Hand configuration after optimizing I_{gq} . (d) Hand configuration after optimizing I_{hc} . (e) Hand configuration after optimizing I_{oe} . (f) Evolution of the quality indexes. The manipulations improving I_{gq} , I_{hc} and I_{oe} ended after 2.122 s and 22 iterations, 5.558 s and 95 iterations and 5.347 s and 65 iterations, respectively. (g) Evolution of the joints values in degrees, q_{11} in blue, q_{12} in red, q_{21} in green, q_{22} in magenta. (h) Average force F_k in Newtons, the dashed line indicates F_d . (i) Evolution of the object orientation in degrees. (j) Angles β_i in degrees, β_1 in blue and β_2 in red (the dashed line indicates the optimal value of β_i). Note that as in Example 3 the contact region is quite small due the object shape and therefore the force F_k cannot reach the desired force. The manipulation ended without reaching the desired object orientation because the friction constraints were not satisfied and the object could slip out of the hand.

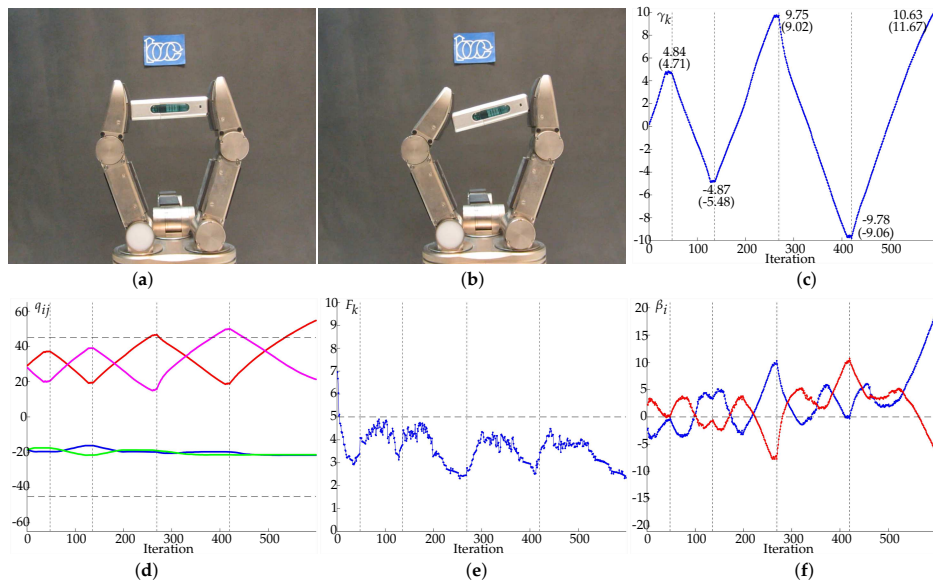


Figure 15. Example 5. (a) Initial grasp. (b) Final grasp. (c) Evolution of the object orientation γ_k with sequential setpoints 5, -5 , 10, -10 and 15 degrees. (d) Evolution of the joints values in degrees, q_{11} in blue, q_{12} in red, q_{21} in green, q_{22} in magenta. (e) Average force F_k in Newtons, the dashed line indicates F_d . (f) Angles β_i in degrees, β_1 in blue and β_2 in red (the dashed line indicates the optimal value of β_i).

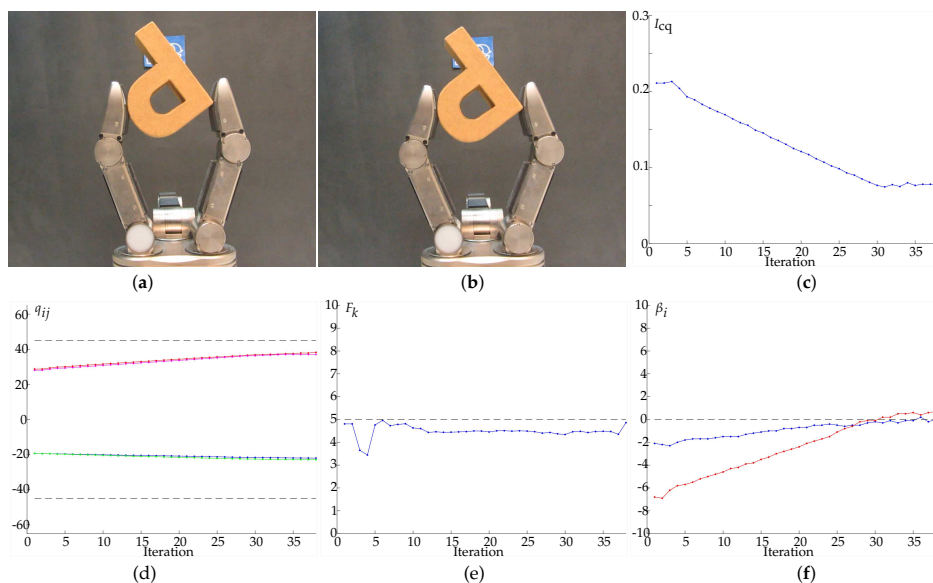


Figure 16. Example 6. (a) Initial grasp. (b) Final grasp. (c) Evolution of the index $I_{cq} = 0.5I_{hc} + 0.5I_{gq}$. (d) Evolution of the joints values in degrees, q_{11} in blue, q_{12} in red, q_{21} in green, q_{22} in magenta. (e) Average force F_k in Newtons, the dashed line indicates F_d . (f) Angles β_i in degrees, β_1 in blue and β_2 in red (the dashed line indicates the optimal value of β_i).

5. Summary and Future Work

This paper has proposed an approach to manipulate unknown objects based on tactile and kinematic information, using two fingers and pursuing three common manipulation goals: the optimization of the hand configuration, the optimization of grasp quality and the optimization of the object orientation. The proposed manipulation strategies can be applied individually or in a combined way. The approach can be applied to different type of robotic hands, since the only

requirements are the knowledge of the hand kinematics, a position control of the fingertips and the availability of tactile information during the manipulation. Note that, in the general case, more degrees of freedom per finger may allow a larger range of manipulation movements.

A natural extension of the proposed approach is the consideration of grasps with more than two fingers, which allow the rotation of the object around any axis. In this case, the system could be underdetermined and it would require a different strategy to adjust the modules of the forces applied by each finger, but the same basic ideas behind each of the manipulations strategies could still be applied. In this sense, note that: (a) moving the fingers to predefined specific configurations is straightforward; (b) movements that potentially improve the grasp quality could be determined if the contact points and the contact force vectors are known (even when this is not evident in the frequent case that the sensors return only the module of the normal component instead of the actual contact force); and (c) finding a (at least approximate) relation between a change in the 3D object orientation and the required finger joint movements looks as a feasible problem by replacing the movements of contact points along a circular path used in this work by movements along a path on spheres centered at some specific point of the object.

From the hardware point of view, this would require fingers with more than two DOF and not all of them producing rotations around parallel axis, in order to avoid hard constraints in the manipulation due to limitations of the joint ranges.

Another topic for future work is the use of the information about the object shape obtained while it is manipulated to optimize the following finger movements. This would help to produce more efficient and smoother movements.

Author Contributions: All authors contributed equally to this work.

Funding: This work was partially supported by the Spanish Government through the project DPI2016-80077-R.

Conflicts of Interest: The authors declare no conflict of interest.

References

1. Bicchi, A. Hands for Dextrous Manipulation and Powerful Grasping: A Difficult Road Towards Simplicity. *IEEE Trans. Robot. Autom.* **2000**, *16*, 652–662. [[CrossRef](#)]
2. Montaña, A.; Suárez, R. Unknown object manipulation based on tactile information. In Proceedings of the IEEE/RSJ International Conference on Intelligent Robots and Systems, Hamburg, Germany, 28 September–2 October 2015; pp. 5642–5647.
3. Bohg, J.; Morales, A.; Asfour, T.; Kragic, D. Data-Driven Grasp Synthesis—A Survey. *IEEE Trans. Robot.* **2014**, *30*, 289–309. [[CrossRef](#)]
4. Miller, A.T.; Allen, P.K. GraspIt!: A Versatile Simulator for Robotic Grasping. *IEEE Robot. Autom. Mag.* **2004**, *11*, 110–122. [[CrossRef](#)]
5. Diankov, R.; Kuffner, J. *OpenRAVE: A Planning Architecture for Autonomous Robotics*; Technical Report July; Robotics Institute, Carnegie Mellon University: Pittsburgh, PA, USA, 2008.
6. Vahrenkamp, N.; Kröhnert, M.; Ulbrich, S.; Asfour, T.; Metta, G.; Dillmann, R.; Sandini, G. Simox: A robotics toolbox for simulation, motion and grasp planning. In *Advances in Intelligent Systems and Computing*; Springer: Berlin/Heidelberg, Germany, 2013; Volume 1, pp. 585–594.
7. Rosales, C.; Suárez, R.; Gabiccini, M.; Bicchi, A. On the synthesis of feasible and prehensile robotic grasps. In Proceedings of the IEEE International Conference on Robotics and Automation, Saint Paul, MN, USA, 14–18 May 2012; pp. 550–556.
8. Cornella, J.; Suarez, R. Efficient Determination of Four-Point Form-Closure Optimal Constraints of Polygonal Objects. *IEEE Trans. Autom. Sci. Eng.* **2009**, *6*, 121–130. [[CrossRef](#)]
9. Prado, R.; Suárez, R. Heuristic grasp planning with three frictional contacts on two or three faces of a polyhedron. In Proceedings of the IEEE International Symposium on Assembly and Task Planning, Montreal, QC, Canada, 19–21 July 2005; Volume 2005, pp. 112–118.
10. Roa, M.A.; Suárez, R. Finding locally optimum force-closure grasps. *Robot. Comput. Integr. Manuf.* **2009**, *25*, 536–544. [[CrossRef](#)]

11. Tovar, N.A.; Suárez, R. Grasp analysis and synthesis of 2D articulated objects with n links. *Robot. Comput. Integr. Manuf.* **2015**, *31*, 81–90. [[CrossRef](#)]
12. Hang, K.; Li, M.; Stork, J.A.; Bekiroglu, Y.; Pokorný, F.T.; Billard, A.; Kragic, D. Hierarchical Fingertip Space: A Unified Framework for Grasp Planning and In-Hand Grasp Adaptation. *IEEE Trans. Robot.* **2016**, *32*, 960–972. [[CrossRef](#)]
13. Przybylski, M.; Asfour, T.; Dillmann, R. Unions of balls for shape approximation in robot grasping. In Proceedings of the IEEE/RSJ International Conference on Intelligent Robots and Systems, Taipei, Taiwan, 18–22 October 2010; pp. 1592–1599.
14. Goldfeder, C.; Allen, P.K. Data-driven grasping. *Auton. Robots* **2011**, *31*, 1–20. [[CrossRef](#)]
15. Li, M.; Hang, K.; Kragic, D.; Billard, A. Dexterous grasping under shape uncertainty. *Robot. Auton. Syst.* **2016**, *75*, 352–364. [[CrossRef](#)]
16. Nogueira, J.; Martínez-Cantin, R.; Bernardino, A.; Jamone, L. Unscented Bayesian optimization for safe robot grasping. In Proceedings of the 2016 IEEE/RSJ International Conference on Intelligent Robots and Systems (IROS), Daejeon, Korea, 9–14 October 2016; pp. 1967–1972.
17. Chen, D.; Dietrich, V.; Liu, Z.; von Wichert, G. A Probabilistic Framework for Uncertainty-Aware High-Accuracy Precision Grasping of Unknown Objects. *J. Intell. Robot. Syst.* **2018**, *90*, 19–43. [[CrossRef](#)]
18. Sommer, N.; Billard, A. Multi-contact haptic exploration and grasping with tactile sensors. *Robot. Auton. Syst.* **2016**, *85*, 48–61. [[CrossRef](#)]
19. Cornellà, J.; Suárez, R.; Carloni, R.; Melchiorri, C. Dual programming based approach for optimal grasping force distribution. *Mechatronics* **2008**, *18*, 348–356. [[CrossRef](#)]
20. Roa, M.A.; Suárez, R. Grasp quality measures: Review and performance. *Auton. Robots* **2014**, *38*, 65–88. [[CrossRef](#)] [[PubMed](#)]
21. Roa, M.A.; Suárez, R.; Cornellà, J. Medidas de calidad para la presión de objetos. *Rev. Iberoam. Autom. Inf. Ind.* **2008**, *5*, 66–82. [[CrossRef](#)]
22. Ferrari, C.; Canny, J. Planning optimal grasps. In Proceedings of the IEEE International Conference on Robotics and Automation, Nice, France, 12–14 May 1992; pp. 2290–2295.
23. Bicchi, A. On the Closure Properties of Robotic Grasping. *Int. J. Robot. Res.* **1995**, *14*, 319–334. [[CrossRef](#)]
24. García, G.J.; Corrales, J.A.; Pomares, J.; Torres, F. Survey of Visual and Force/Tactile Control of Robots for Physical Interaction in Spain. *Sensors* **2009**, *9*, 9689–9733. [[CrossRef](#)] [[PubMed](#)]
25. Zou, L.; Ge, C.; Wang, Z.J.; Cretu, E.; Li, X. Novel Tactile Sensor Technology and Smart Tactile Sensing Systems: A Review. *Sensors* **2017**, *17*. [[CrossRef](#)] [[PubMed](#)]
26. Kappasov, Z.; Corrales-Ramón, J.A.; Perdereau, V. Tactile sensing in dexterous robot hands—Review. *Robot. Auton. Syst.* **2015**, *74*, 195–220. [[CrossRef](#)]
27. Bekiroglu, Y.; Detry, R.; Kragic, D. Learning Tactile Characterizations Of Object-And Pose-specific Grasps. In Proceedings of the IEEE/RSJ International Conference on Intelligent Robots and Systems, San Francisco, CA, USA, 25–30 September 2011; pp. 1554–1560.
28. Dang, H.; Weisz, J.; Allen, P.K. Blind grasping: Stable robotic grasping using tactile feedback and hand kinematics. In Proceedings of the IEEE International Conference on Robotics and Automation, Shanghai, China, 9–13 May 2011; pp. 5917–5922.
29. Boutselis, G.I.; Bechlioulis, C.P.; Liarokapis, M.; Kyriakopoulos, K.J. An integrated approach towards robust grasping with tactile sensing. In Proceedings of the IEEE International Conference on Robotics and Automation, Hong Kong, China, 31 May–7 June 2014; pp. 3682–3687.
30. Montaña, A.; Suárez, R. Object shape reconstruction based on the object manipulation. In Proceedings of the IEEE International Conference on Advanced Robotics, Montevideo, Uruguay, 25–29 November 2013; pp. 1–6.
31. Jara, C.A.; Pomares, J.; Candelas, F.A.; Torres, F. Control Framework for Dexterous Manipulation Using Dynamic Visual Servoing and Tactile Sensors’ Feedback. *Sensors* **2014**, *14*, 1787–1804. [[CrossRef](#)] [[PubMed](#)]
32. Cole, A.B.A.; Hauser, J.E.; Sastry, S.S. Kinematics and control of multifingered hands with rolling contact. *IEEE Trans. Autom. Control* **1989**, *34*, 398–404. [[CrossRef](#)]
33. Li, Q.; Haschke, R.; Ritter, H.; Bolder, B. Towards unknown objects manipulation. *IFAC Proc. Volumes* **2012**, *45*, 289–294. [[CrossRef](#)]
34. Song, S.K.; Park, J.B.; Choi, Y.H. Dual-fingered stable grasping control for an optimal force angle. *IEEE Trans. Robot.* **2012**, *28*, 256–262. [[CrossRef](#)]

35. Platt, R. Learning and Generalizing Control-Based Grasping and Manipulation Skills. Ph.D. Thesis, University of Massachusetts Amherst, Amherst, MA, USA, 2006.
36. Tahara, K.; Arimoto, S.; Yoshida, M. Dynamic object manipulation using a virtual frame by a triple soft-fingered robotic hand. In Proceedings of the IEEE International Conference on Robotics and Automation, Anchorage, AK, USA, 3–7 May 2010; pp. 4322–4327.
37. MacKenzie, C.L.; Iberall, T. *The Grasping Hand*; Elsevier: New York, NY, USA, 1994; Volume 104, p. 482.
38. Chang, L.Y.; Pollard, N.S. Video survey of pre-grasp interactions in natural hand activities. In RSS Workshop: Understanding the Human Hand for Advancing Robotic Manipulation, Seattle, WA, USA, 28 June– 1 July 2009; pp. 1–2.
39. Toh, Y.P.; Huang, S.; Lin, J.; Bajzek, M.; Zeglin, G.; Pollard, N.S. Dexterous telemanipulation with a multi-touch interface. In Proceedings of the IEEE-RAS International Conference on Humanoid Robots, Osaka, Japan, 29 November–1 December 2012; pp. 270–277.
40. Nguyen, V.D. Constructing Force- Closure Grasps. *Int. J. Robot. Res.* **1988**, *7*, 3–16. [[CrossRef](#)]
41. Wörn, H.; Haase, T. Force approximation and tactile sensor prediction for reactive grasping. In Proceedings of the World Automation Congress, Puerto Vallarta, Mexico, 24–28 June 2012; pp. 1–6.
42. Liégeois, A. Automatic Supervisory Control of the Configuration and Behavior of Multibody Mechanisms. *IEEE Trans. Syst. Man Cybern.* **1977**, *7*, 868–871.
43. Ozawa, R.; Arimoto, S.; Nguyen, P.; Yoshida, M.; Bae, J.H. Manipulation of a circular object in a horizontal plane by two finger robots. In Proceedings of the 2004 IEEE International Conference on Robotics and Biomimetics, Shenyang, China, 22–26 August 2004; pp. 517–522.
44. Montañó, A.; Suárez, R. Commanding the object orientation using dexterous manipulation. In *Advances in Intelligent Systems and Computing*; Springer Verlag: Berlin, Germany, 2016; Volume 418, pp. 69–79.
45. Tomo, T.P.; Schmitz, A.; Wong, W.K.; Kristanto, H.; Somlor, S.; Hwang, J.; Jamone, L.; Sugano, S. Covering a Robot Fingertip With uSkin: A Soft Electronic Skin With Distributed 3-Axis Force Sensitive Elements for Robot Hands. *IEEE Robot. Autom. Lett.* **2018**, *3*, 124–131. [[CrossRef](#)]



© 2018 by the authors. Licensee MDPI, Basel, Switzerland. This article is an open access article distributed under the terms and conditions of the Creative Commons Attribution (CC BY) license (<http://creativecommons.org/licenses/by/4.0/>).